Inorganic Chemistry
Article

Inorg. Chem. **2010**, *49*, 2851–2858 **2851**
DOI: 10.1021/ic902341w

Structural, Magnetic, EPR, and Electrochemical Characterizations of a Spin-Frustrated Trinuclear Cr^{III} Polyoxometalate and Study of Its Reactivity with Lanthanum Cations

Jean-Daniel Compain,[†] Pierre Mialane,*[,†] Anne Dolbecq,[†] Israël Martyr Mbomekallé,[†] Jérôme Marrot,[†] Francis Sécheresse,[†] Carole Duboc,[‡] and Eric Rivière[§]

[†]*Institut Lavoisier de Versailles, UMR CNRS 8180, Université de Versailles Saint Quentin, 78035 Versailles Cedex, France,* [‡]*Université Joseph Fourier Grenoble 1/CNRS, Département de Chimie Moléculaire, UMR 5250, Institut de Chimie Moléculaire de Grenoble, FR-CNRS-2607, BP 53, 38041 Grenoble Cedex 9, France, and* [§]*Institut de Chimie Moléculaire et des Matériaux d'Orsay, UMR 8182, Equipe Chimie Inorganique, Univ. Paris-Sud, 91405 Orsay cedex, France*

Received November 26, 2009

The asymmetric Cr^{III} polyoxometalate complex $Cs_{10}[(\gamma\text{-}SiW_{10}O_{36})_2(Cr(OH)(H_2O))_3]\cdot 17H_2O$ (**1**) has been synthesized in water under atmospheric pressure from the trinuclear precursor $[Cr_3(CH_3COO)_7(OH)_2]$ and the divacant ligand $[\gamma\text{-}SiW_{10}O_{36}]^{8-}$. Complex **1** is built up of two $[\gamma\text{-}SiW_{10}O_{36}]^{8-}$ Keggin units sandwiching a trinuclear $\{(Cr^{III}(OH)(H_2O))_3\}$ fragment where the paramagnetic centers are bridged by three μ-OH ligands forming a nearly isosceles triangle. The magnetic properties of this spin-frustrated system have thus been interpreted considering a 2-*J* Hamiltonian showing that the Cr^{III} ions are antiferromagnetically coupled and that **1** possesses an $S = 3/2$ ground state with an $S = 1/2$ first excited state located at 11 cm^{-1}. These results have been confirmed by EPR spectroscopy measurements (Q-band), which have also enabled the quantification of the electronic parameters characterizing the quadruplet spin ground state. The magnitude of the magnetic exchange interactions and the nature of the ground state are discussed in light of previously reported isosceles triangular $S = 3/2$ clusters. UV−visible and electrochemical studies have shown that **1** is stable in aqueous media in a 1−7 pH range. This stability is chemically confirmed by the study of the reactivity of **1** with La^{III} cations, which has allowed the isolation of the $Cs_4[(\gamma\text{-}SiW_{10}O_{36})_2(Cr(OH)(H_2O))_3(La(H_2O)_7)_2]\cdot 20H_2O$ compound (**2**). Indeed, during the synthetic process of this 3d−4f system, the integrity of the $[(\gamma\text{-}SiW_{10}O_{36})_2(Cr(OH)(H_2O))_3]^{10-}$ building unit constituting **1** is maintained despite the high oxophilic character of the La^{III} ions. The single crystal X-ray diffraction study of **2** has revealed that in the solid state the rare earth cations connect these subunits, affording a 3d−4f double-chain monodimensional system.

Introduction

While the implication of polyoxometalate (POM) compounds in fields such as catalysis[1] or analysis[2] has been evidenced for several decades, the relevance of these molecular oxides in molecular magnetism has been clearly underlined only in the course of the 1990s.[3] Even if the family of the polyoxovanadate complexes has been widely investigated,[4] in the huge majority of cases, the studied complexes have been prepared from vacant polyoxotungstates and 3d metal centers. Focusing on polyoxotungstate systems, complexes encapsulating from one to 28[5] 3d paramagnetic centers have been characterized. These compounds can be pure metal oxide/hydroxide systems. However, the introduction of exogenous bridging ligands such as acetate or azide in the inorganic matrix leads to compounds presenting magnetic properties which can differ from those characterizing organic ligand/3d metal complexes with similar bridging ligands.[6] In POM systems, the magnetic core is encapsulated by the bulky diamagnetic polyoxotungstate framework leading to an effective isolation of the magnetic fragment which allows

*To whom correspondence should be addressed. Fax: (+33)-1-39254381. E-mail: mialane@chimie.uvsq.fr.

(1) (a) Rudenkov, A. I.; Mennenga, G. U.; Rachkovskaya, L. N.; Mateev, K. I.; Kozhevnikov, I. V. *Kinet. Katal.* **1977**, *18*, 758. (b) Mizuno, N.; Misono, N. *Chem. Rev.* **1998**, *98*, 199. (c) Neumann, R. *Prog. Inorg. Chem.* **1998**, *47*, 317. (d) Hill, C. L., Ed. *J. Mol. Catal. A.: Chem.* **2007**, *262*, 1−242; Polyoxometalate in Catalysis.

(2) Williams, W. J. *Handbook of Anion Determination*; Butterworths: London, 1979.

(3) Clemente-Juan, J. M.; Coronado, E. *Coord. Chem. Rev.* **1999**, *193*−*195*, 361.

(4) Müller, A.; Peters, F.; Pope, M. T.; Gatteschi, D. *Chem. Rev.* **1998**, *98*, 239.

(5) Godin, B.; Chen, Y.-G.; Vaissermann, J.; Ruhlmann, L.; Verdaguer, M.; Gouzerh, P. *Angew. Chem., Int. Ed.* **2005**, *44*, 3072.

(6) Mialane, P.; Dolbecq, A.; Sécheresse, F. *Chem. Commun.* **2006**, 3477.

Published on Web 02/10/2010

the accurate determination of the intramolecular magnetic exchange interactions. Moreover, it has recently been shown that polynuclear transition metal POM clusters can behave as single molecule magnets (SMMs).[7] The reported POM SMMs contain manganese[7a] or iron[7b] centers, two types of 3d cations which have been particularly considered for the elaboration of magnetic POMs. Furthermore, the synthesis of nickel, cobalt, and copper POMs has also been widely investigated. In contrast, the chemistry of chromium POMs remains far less developed due to the difficulty of obtaining characterizable POM compounds with such paramagnetic ions.

In 1994, Wassermann and Lunk reported the crystal structure of the monomeric $[A\text{-}\alpha\text{-}SiW_9O_{34}(Cr(OH)(H_2O))_3]^{4-}$ polyanion[8] (Figure SI1a, Supporting Information) previously synthesized by Peng et al.[9] In this compound, a triangular $\{Cr^{III}\}_3$ fragment where the paramagnetic centers are connected by hydroxo groups is inserted in the trivacant $[A\text{-}\alpha\text{-}SiW_9O_{34}]^{10-}$ ligand. The year after, the same group reported on the dimeric $(NH_4)_{11}[\{A\text{-}\alpha\text{-}SiW_9O_{34}(Cr(OH)(H_2O))_3\}_2(OH)_3]\cdot 23H_2O$ POM with a hexanuclear Cr^{III} core (Figure SI1b, Supporting Information).[10] This complex can be seen as the dimerized form of the monomeric Cr^{III} complex mentioned above, the connection between the two $[A\text{-}\alpha\text{-}SiW_9O_{34}(Cr(OH)(H_2O))_3]^{4-}$ units being ensured by three additional μ-OH groups substituting the six terminal water molecules of two $\{Cr^{III}\}_3$ subunits. Finally, in 1996, the $[\gamma\text{-}SiW_{10}O_{36}Cr_2(H_2O)_2(OH)(CH_3COO)_2]^{5-}$ polyanion which contains a dinuclear complex was reported (Figure SI1c, Supporting Information).[11] In this compound, the two Cr^{III} centers are bridged by two acetato ligands and a hydroxo group. The paramagnetic centers share a corner, and the $[\gamma\text{-}SiW_{10}O_{36}]^{8-}$ part acts as a tetradentate ligand. Besides these three compounds, to the best of our knowledge, no other Cr^{III} complex structured by vacant polyoxotungstates has been reported. However, we can mention the extensive study performed by Mizuno et al. who has shown that $[\alpha\text{-}XW_{12}O_{40}]^{n-}$ ($X = P^V, Si^{IV}, B^{III}, ...$; $n = 3-6$) saturated Keggin ions can form ionic crystals with $[Cr_3O(OOCR)_6(H_2O)_3]^+$ ($R = H, CH_3$) trinuclear species, these hybrid materials exhibiting very interesting guest sorption properties.[12]

We present here our first results concerning the reaction of the trinuclear, neutral precursor $[Cr_3(CH_3COO)_7(OH)_2]$ with a vacant polyoxotungstate. The silicotungstate POM $[\gamma\text{-}SiW_{10}O_{36}]^{8-}$, which has been widely used as precursor in synthetic POM chemistry[13] especially due to the catalytic properties of this anion and of the corresponding 3d-functionalized derivatives,[14] has been considered as the ligand. The complex $Cs_{10}[(\gamma\text{-}SiW_{10}O_{36})_2(Cr(OH)(H_2O))_3]\cdot 17H_2O$ (**1**) has been isolated, and the quantification of magnetic exchange interactions occurring between Cr^{III} centers embedded in a POM matrix is reported here for the first time. The nature of the ground state characterizing this spin frustrated system[15] has been confirmed by EPR spectroscopy, and the stability of this compound has been stated *via* electronic absorption spectroscopy and electrochemical experiments. Finally, the reactivity of complex **1** with La^{III} cations has been studied, leading to the isolation of the monodimensional $Cs_4[(\gamma\text{-}SiW_{10}O_{36})_2(Cr(OH)(H_2O))_3(La(H_2O)_7)_2]\cdot 20H_2O$ (**2**) compound, which has been structurally characterized.

Experimental Section

Chemicals and Reagents. The lacunary precursor $K_8[\gamma\text{-}SiW_{10}O_{36}]\cdot 12H_2O$ was synthesized as previously described.[16] All other chemicals were used as purchased without purification, including the $[Cr_3(CH_3COO)_7(OH)_2]$ trinuclear chromium(III) acetate hydroxide compound (Aldrich).

Synthesis of $Cs_{10}[(\gamma\text{-}SiW_{10}O_{36})_2(Cr(OH)(H_2O))_3]\cdot 17H_2O$ (1). In 40 mL of water were dissolved 2 g (0.67 mmol) of $K_8[\gamma\text{-}SiW_{10}O_{36}]\cdot 12H_2O$ and 400 mg (0.66 mmol) of $[Cr_3(CH_3COO)_7(OH)_2]$. The mixture was let stirring for 1.5 h at 80 °C, then allowed to cool down to room temperature before 1 g of CsCl (5.94 mmol) was added. The solution was left stirring for another 30 min at room temperature. During this time, a green powder slowly precipitated. The powder was filtrated over a fine frit and dried with ethanol and diethyl ether. Yield: 715 mg (31% based on W). The crude powder can be dissolved in the minimal amount of warm water, the slow evaporation of this solution affording small green crystals the day after. Anal. Calcd for $W_{20}Cr_3Cs_{10}Si_2O_{95}H_{43}$ (found): W 54.22 (54.41), Cr 2.30 (2.27), Si 0.83 (1.18), Cs 19.60 (18.89). IR (KBr pellets) cm^{-1}: 1048 (m), 994 (m), 949 (m), 895 (s), 873 (s), 823 (m), 751 (s), 604 (m), 528 (m), 484 (w). Electronic spectral data obtained in H_2O, λ_{max}, nm (ε, L mol^{-1} cm^{-1}): 468 (680), 627 (160).

Synthesis of $Cs_4[(\gamma\text{-}SiW_{10}O_{36})_2(Cr(OH)(H_2O))_3(La(H_2O)_7)_2]\cdot 20H_2O$ (2). A total of 200 mg (0.03 mmol) of complex **1** was dissolved in 7 mL of warm water before 65 mg (0.18 mmol) of $LaCl_3\cdot 7H_2O$ was added. The mixture was left stirring at 80 °C for 2 h then allowed to cool down to room temperature. After the fine light green powder was eliminated by centrifugation, the resulting solution was left to evaporate at room temperature, affording small light green crystals after a few hours. Yield: 81 mg (41% based on **1**). Anal. Calcd for $La_2W_{20}Cr_3Cs_4Si_2O_{112}H_{77}$ (found): W 56.13 (56.00), Cr 2.38 (2.40), Si 0.86 (1.21), Cs 8.11 (7.25), La 4.24 (4.51), H 1.15 (1.14). IR (KBr pellets), cm^{-1}: 1048 (m), 1001 (m), 955 (m), 915 (sh), 879 (s), 802 (m), 751 (m), 604 (m), 534 (m), 484 (w). Electronic spectral data obtained in H_2O, λ_{max}, nm (ε, L mol^{-1} cm^{-1}): 462 (570), 629 (150).

X-Ray Crystallography. Intensity data collections were carried out at room temperature with a Siemens SMART three-circle diffractometer. The absorption correction was based on multiple and symmetry-equivalent reflections in the data set using the SADABS program[17] based on the method of Blessing.[18] The structures were solved by direct methods and refined

(7) (a) Ritchie, C.; Ferguson, A.; Nojiri, H.; Miras, H. N.; Song, Y.-F.; Long, D.-L.; Burkholder, E.; Murrie, M.; Kögerler, P.; Brechin, E. K.; Cronin, L. *Angew. Chem., Int. Ed.* **2008**, *47*, 5609. (b) Compain, J.-D.; Mialane, P.; Dolbecq, A.; Mbomekalle, I. M.; Marrot, J.; Sécheresse, F.; Rivière, E.; Rogez, G.; Wernsdorfer, W. *Angew. Chem., Int. Ed.* **2009**, *48*, 3077.
(8) Wassermann, K.; Lunk, H.-J. *Acta Crystallogr.* **1994**, *C50*, 348.
(9) Peng, J.; Qu, L.; Chen, Y. *Inorg. Chim. Acta* **1991**, *183*, 157.
(10) Wassermann, K.; Palm, R.; Lunk, H.-J.; Fuchs, J.; Steinfeldt, N.; Stösser, R. *Inorg. Chem.* **1995**, *34*, 5029.
(11) Wasserman, K.; Lunk, H.-J.; Palm, R.; Fuchs, J.; Steinfeldt, N.; Stösser, R.; Pope, M. T. *Inorg. Chem.* **1996**, *35*, 3273.
(12) Uchida, S.; Mizuno, N. *Coord. Chem. Rev.* **2007**, *251*, 2537.
(13) See for example: (a) Botar, B.; Kögerler, P. *Dalton Trans.* **2008**, 3150. (b) Bi, L.-H.; Chubarova, E. V.; Nsouli, N. H.; Dickman, M. H.; Kortz, U.; Keita, B.; Nadjo, L. *Inorg. Chem.* **2006**, *45*, 8575.
(14) (a) Kikukawa, Y.; Yamaguchi, S.; Nakagawa, Y.; Uehara, K.; Uchida, S.; Yamaguchi, K.; Mizuno, N. *J. Am. Chem. Soc.* **2008**, *130*, 15872. (b) Kamata, K.; Nakagawa, Y.; Yamaguchi, K.; Mizuno, N. *J. Am. Chem. Soc.* **2008**, *130*, 15304. (c) Botar, B.; Geletii, Y. V.; Kögerler, P.; Musaev, D. G.; Morokuma, K.; Weinstock, I. A.; Hill, C. L. *J. Am. Chem. Soc.* **2006**, *128*, 11268.
(15) For a recent review devoted to the spin-frustration phenomenon in polyoxometalates, see: Kögerler, P.; Tsukerblat, B.; Müller, A. *Dalton Trans.* **2010**, *39*, 21.
(16) Tézé, A.; Hervé, G. *Inorg. Synth.* **1990**, *27*, 85.
(17) Sheldrick, G. M. *SADABS*; University of Göttingen: Göttingen, Germany, 1997.
(18) Blessing, R. *Acta Crystallogr.* **1995**, *A51*, 33.

Table 1. Crystallographic Data for Compounds **1** and **2**

	1	**2**
empirical formula	$W_{20}Cr_3Cs_{10}Si_2O_{95}H_{43}$	$La_2W_{20}Cr_3Cs_4Si_2O_{111}H_{75}$
fw, g	6781.32	6549.94
temperature, K	293(2)	293(2)
cryst syst	triclinic	triclinic
space group	$P\bar{1}$	$P\bar{1}$
a/Å	12.523(3)	12.7643(6)
b/Å	19.263(4)	19.2319(9)
c/Å	19.756(5)	21.1546(10)
α/deg	98.031(6)	78.0490(10)
β/deg	98.362(6)	89.2950(10)
γ/deg	106.566(7)	71.4010(10)
V/Å^3	4436.2(18)	4807.1(4)
Z	2	2
ρ_{calc}/g cm^{-3}	5.144	4.538
μ/mm^{-1}	30.360	26.659
data/params	25213/1084	16852/1102
R_{int}	0.0660	0.0499
GOF	0.968	1.025
R ($>2\sigma(I)$)	$R_1{}^a$ = 0.0747 $wR_2{}^b$ = 0.1761	R_1 = 0.0629 wR_2 = 0.1654

$^a R_1 = (\sum||F_o| - |F_c||)/\sum|F_c|$. $^b wR2 = \sqrt{[\sum(F_o^2 - F_c^2)^2/\sum w(F_o^2)^2]}$.

by full-matrix least-squares using the SHELX-TL package.[19] In **1** and **2** there is a discrepancy between the formulas determined by elemental analysis and the formulas deduced from the crystallographic atom list because of the difficulty in locating all the disordered water molecules. Crystallographic data are given in Table 1. Selected bond lengths for **1** and **2** are given in Tables SI1 and Table SI2 (Supporting Information), respectively.

Elemental analyses were performed by the Service Central d'Analyse of CNRS, 69390 Vernaison, France.

Thermogravimetry was carried out under a nitrogen flow (20 mL/min) with a Perkin-Elmer electrobalance TGA-7 at a heating rate of 5 °C/min up to 600 °C.

Infrared spectra (KBr pellets) were recorded on an IRFT Nicolet 550 apparatus.

EPR Spectroscopy. Q-band EPR spectra were recorded with a Bruker EMX, equipped with the ER-5106 QTW Bruker cavity and an Oxford Instruments ESR-900 continuous-flow helium cryostat.

Magnetic Properties. Magnetic susceptibility measurements were carried out with a Quantum Design SQUID Magnetometer with an applied field of 1000 G using powder samples pressed in pellets to avoid preferential orientation of the crystallites. The independence of the susceptibility value with regard to the applied field was checked at room temperature. The susceptibility data were corrected from the diamagnetic contributions as deduced by using Pascal's constant tables. The susceptibility times temperature as a function of temperature curve has been simulated using MAGPACK.[20] The magnetizations as a function of the magnetic field curves have been fitted by full diagonalization of the Hamiltonian.

UV−Visible Spectroscopy and Electrochemical Experiments. Pure water was used throughout. It was obtained by passing it through a RiOs 8 unit followed by a Millipore-Q Academic purification set. All reagents were of high-purity grade and used as purchased without further purification. The UV−visible spectra were recorded on a Perkin-Elmer Lambda 19 spectrophotometer with 10^{-4} or 10^{-3} M solutions of the relevant polyanion. Matched 1.000 cm optical path length quartz cuvettes were used. The compositions of the various media were as follows: for pH 1 and 3, 0.2 M $Na_2SO_4 + H_2SO_4$; for pH 5, 0.4 M $CH_3COONa + CH_3COOH$; for pH 7, 0.4 M NaH_2PO_4 + NaOH.

The same media as for UV−visible spectroscopy were used for electrochemistry, but the polyanion concentration was 0.2 mM. All cyclic voltammograms were recorded at a scan rate of 10 mV s^{-1} unless otherwise stated. The solutions were deaerated thoroughly for at least 30 min, with pure argon, and kept under a positive pressure of this gas during the experiments. The source, mounting, and polishing of the glassy carbon (GC, Carbone Lorraine, France) electrodes has been described.[21] The glassy carbon samples had a diameter of 3 mm. Controlled potential coulometry experiments were performed using a large surface area glassy carbon plate as working electrode. The auxiliary electrode was a Pt plate placed within a fritted-glass isolation chamber. Potentials are quoted against a saturated calomel electrode (SCE). The electrochemical setup was an EG&G 273 A driven by a PC with the M270 software. All experiments were performed at room temperature.

Results and discussion

Synthesis. The $Cs_{10}[(\gamma\text{-}SiW_{10}O_{36})_2(Cr(OH)(H_2O))_3]\cdot 17H_2O$ complex **1** has been synthesized by mixing in water at 80 °C the potassium salt of the divacant ligand $[\gamma\text{-}SiW_{10}O_{36}]^{8-}$ with the trinuclear cluster $[Cr_3(CH_3COO)_7(OH)_2]$. While previous studies have shown that in the presence of 3d cations the $[\gamma\text{-}SiW_{10}O_{36}]^{8-}$ divacant ligand can decompose to tri- or tetravacant ligands even at room temperature,[22] be isomerized,[13a,23] or lead to the dimerized species $[M(\gamma\text{-}SiW_{10}O_{35})_2]^{10-}$ ($M = Co^{II}, Mn^{II}, Ni^{II}$),[24] the structure of the POM precursor is preserved during the synthetic process of **1**, as previously found for several M-substituted silicodecatungstate systems (M = Fe,[14c] Zr,[25] Hf,[25] Cu,[14b,22c] etc.). The retention of the $[\gamma\text{-}SiW_{10}O_{36}]^{8-}$ unit suggests that the formation of **1** is rapid. Moreover, **1** is stable in an aqueous medium even under heating at reflux, indicating that **1** is inert, like numerous reported Cr^{III} complexes. Redissolution of complex **1** in hot water (80 °C) followed by the addition of an excess of La^{3+} cations afforded the 3d−4f $Cs_4[(\gamma\text{-}SiW_{10}O_{36})_2(Cr(OH)(H_2O))_3(La(H_2O)_7)_2]\cdot 19H_2O$ compound **2**. Considering the strong oxophilic character of rare earth cations compared to 3d metals,[26] this experiment also confirms the stability of the $[(\gamma\text{-}SiW_{10}O_{36})_2(Cr(OH)(H_2O))_3]^{10-}$ fragment and shows that in the solid state these building units can be organized by 4f centers acting as connectors. The electronic absorption spectrum of **1** in water presents two main bands in the visible domain (Figure SI2a, Supporting Information). Considering that the Cr^{III} centers are weakly coupled at room temperature (see below), it can be tentatively

(19) Sheldrick, G. M. *SHELX-TL*, version 5.03; Siemens Analytical X-ray Instrument Division: Madison, WI, 1994.
(20) Borras-Almenar, J. J.; Clemente-Juan, J. M.; Coronado, E.; Tsukerblat, B. S. *J. Comput. Chem.* **2001**, *22*, 985.
(21) Keita, B.; Nadjo, L. *J. Electroannal. Chem.* **1988**, *243*, 87.
(22) (a) Lisnard, L.; Mialane, P.; Dolbecq, A.; Marrot, J.; Clemente-Juan, J. M.; Coronado, E.; Keita, B.; de Oliveira, P.; Nadjo, L.; Sécheresse, F. *Chem.—Eur. J.* **2007**, *13*, 3525. (b) Bassil, B. S.; Kortz, U.; Tigan, A. S.; Clemente-Juan, J. M.; Keita, B.; de Oliveira, P.; Nadjo, L. *Inorg. Chem.* **2005**, *44*, 2659. (c) Mialane, P.; Dolbecq, A.; Marrot, J.; Rivière, E.; Sécheresse, F. *Chem.—Eur. J.* **2005**, *11*, 1771.
(23) Kortz, U.; Jeannin, Y. P.; Tézé, A.; Hervé, G.; Isber, S. *Inorg. Chem.* **1999**, *38*, 3670.
(24) Bassil, B. S.; Dickman, M. H.; Reicke, M.; Kortz, U.; Keita, B.; Nadjo, L. *Dalton Trans.* **2006**, 4253.
(25) Kikukawa, Y.; Yamaguchi, S.; Tsuchida, K.; Nakagawa, Y.; Uehara, K.; Yamaguchi, K.; Mizuno, N. *J. Am. Chem. Soc.* **2008**, *130*, 5472.
(26) Nohra, B.; Mialane, P.; Dolbecq, A.; Rivière, E.; Marrot, J.; Sécheresse, F. *Chem. Commun.* **2009**, 2703.

interpreted that the paramagnetic centers are isolated.[27] The $^4A_{2g}(F) \rightarrow {}^4T_{2g}(F)$ transition is observed at 630 nm, while the $^4A_{2g}(F) \rightarrow {}^4T_{1g}(F)$ transition is located at 470 nm, leading to the spectral parameters Δ_0 = 15 900 cm^{-1} and B (Racah parameter) = 530 cm^{-1}.[28] Additionally, a shoulder at 725 nm can be ascribed to spin-forbidden transition(s) involving excited doublet spin state(s). The $^4A_{2g}(F) \rightarrow {}^4T_{2g}(P)$ band, expected at ca. 300 nm, is masked by the intense O → W charge transfer bands of the inorganic ligand which appears as a shoulder at ca. 265 nm ($\varepsilon \approx 40\,000$ L mol^{-1} cm^{-1}). As expected, the UV−visible spectrum of the soluble compound **2** is similar to that described for complex **1** (Figure SI2b, Supporting Information). TGA have been performed on **1** and **2**. For compound **1** (Figure SI3a, Supporting Information), a weight loss of 5.7% corresponding to the departure of the free and coordinated water molecules is observed when the temperature is increased from room temperature to 400 K. This is in full agreement with the calculated value of 5.6%. For compound **2** (Figure SI3b, Supporting Information), the calculated value (10.2%) is also in agreement with the experimental one (9.9%). Finally, attempts at synthesizing **1** using a mononuclear chromium precursor salt have failed, showing that, even if the trinuclear $[Cr_3(CH_3COO)_7(OH)_2]$ complex decomposes during the formation of **1**, the choice of the 3d metallic precursor is crucial.

Structure of Compound $Cs_{10}[(\gamma\text{-}SiW_{10}O_{36})_2(Cr(OH)(H_2O))_3]\cdot 17H_2O$ (1). Complex **1** is built up of two $[\gamma\text{-}SiW_{10}O_{36}]^{8-}$ Keggin units sandwiching a trinuclear $\{(Cr^{III}(OH)(H_2O))_3\}$ fragment (Figure 1). Two Cr^{III} centers are each coordinated to two terminal W=O oxygen atoms of a $[\gamma\text{-}SiW_{10}O_{36}]^{8-}$ ligand, forming an "out-of-pocket" $\{SiW_{10}Cr_2\}$ monomeric unit. Such a coordination mode has previously been observed in Cr^{III},[11] Fe^{III},[14c,29] and Ru^{IV} [30] POMs. Additionally, each of these two Cr^{III} paramagnetic centers is connected *via* one W=O oxygen of the other divacant polyanion constituting **1**, ensuring the connection of the two $[\gamma\text{-}SiW_{10}O_{36}]^{8-}$ subunits. The third chromium center is connected to only one divacant Keggin unit, this cation being tricoordinated to this subunit *via* two W=O oxygen centers and an oxygen atom of the heterometallic $\{SiO_4\}$ group. Three μ-OH ligands (BVS(μ_3-O(H)) = 1.03, 1.08, and 1.14)[31] bridge the Cr^{III} ions (1.914(15) ≤ d_{Cr-OH} ≤ 1.971(16) Å), allowing the formation of a nearly isosceles triangular cluster $\{(Cr^{III}(OH)(H_2O))_3\}$ with Cr···Cr distances of 3.610(6), 3.613(6), and 3.723(6) Å. A terminal water molecule (BVS(H_2O) = 0.408, 0.428, 0.465) completes the coordination sphere of each paramagnetic center, which thus adopts a slightly axially distorted octahedral arrangement. Such a $\{(Cr^{III}(OH)(H_2O))_3\}$ fragment is close to that observed in the monomeric $[A\text{-}\alpha\text{-}SiW_9O_{34}(Cr(OH)(H_2O))_3]^{4-}$ polyanion.[8] Nevertheless, this last compound possesses a pseudo C_{3v} symmetry, the Cr^{III} centers forming a nearly equilateral triangle with Cr···Cr distances of 3.603(9) and 3.620(9) Å. Noticeably, except for the latter, no other example of a complex possessing a $\{(Cr^{III}(OH))_3\}$ core had been reported. Indeed, the chemistry of $\{Cr^{III}{}_3\}$ triangular complexes is strongly dominated by oxo-centered systems, with additional carboxylato ligands connecting the 3d centers.[32] Also, as observed in the $[\{Ru_4O_4(OH)_2(H_2O)_4\}(\gamma\text{-}SiW_{10}O_{36})_2]^{10-}$ complex,[30] the two $\{SiW_{10}\}$ units are rotated by 90°, with a "slipped" configuration comparable to the one found in the organometallic $[(C_6H_5SnOH_2)_2(\gamma\text{-}SiW_{10}O_{36})_2]^{10-}$ compound.[33] Obviously, contrary to these complexes, no C_2 axis can be observed in **1** due to the presence of the $\{(Cr^{III}(OH)(H_2O))_3\}$ trinuclear fragment, the title compound possessing only a pseudo-mirror plane passing through the silicon atoms and the Cr(2) center (see Figure 1). Consequently, **1** adopts an overall pseudo C_s symmetry.

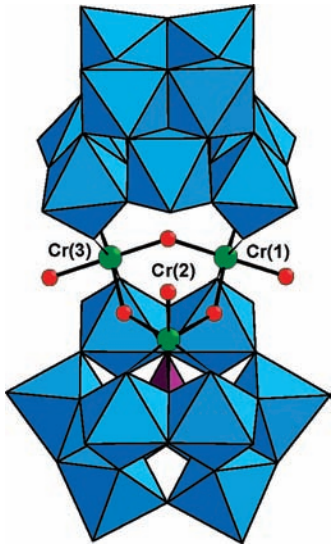

Figure 1. Polyhedral and ball-and-stick representation of the $[(\gamma\text{-}SiW_{10}O_{36})_2(Cr(OH)(H_2O))_3]^{10-}$ polyanion in **1**. Blue octahedra, $\{WO_6\}$; green spheres, Cr; red spheres, O; purple tetrahedra, $\{SiO_4\}$.

Structure of Compound $Cs_4[(\gamma\text{-}SiW_{10}O_{36})_2(Cr(OH)(H_2O))_3(La(H_2O)_7)_2]\cdot 19H_2O$ (2). Compound **2** (Figure 2) adopts a 1D arrangement arising from the connection by La^{III} cations of $[(\gamma\text{-}SiW_{10}O_{36})_2(Cr(OH)(H_2O))_3]^{10-}$ subunits analogous to those found in the unit cell of complex **1**. Two crystallographically independent rare earth centers, labeled La(1) and La(2), are present in the crystal structure of **2**. Each La(1) center connects two $[(\gamma\text{-}SiW_{10}O_{36})_2(Cr(OH)(H_2O))_3]^{10-}$ subunits *via* two W=O···La(1) bonds (d_{La-O} 2.537(15) and 2.591(12) Å), leading to infinite $\{La(\gamma\text{-}SiW_{10}O_{36})_2(Cr(OH)(H_2O))_3\}_\infty$ linear chains. Moreover, two adjacent chains are connected by the La(2) centers *via* two W=O···La(2) bonds (d_{La-O} 2.504(14) and 2.604(15) Å), affording a double-chain monodimensional system. The coordination spheres of La(1) and La(2) are both completed by seven terminal water molecules (see Table SI2, Supporting Information) leading to nonacoordinated rare earth centers, which adopt distorted tricapped trigonal prismatic arrangements. The first report dealing with the elaboration of systems where sandwich-type

(27) Güdel, H. U.; McCarthy, P. J. *Coord. Chem. Rev.* **1988**, *88*, 69.
(28) Lever, A. B. P. *Inorganic Electronic Spectroscopy*, 2nd ed.; Elsevier: Amsterdam, 1984.
(29) Botar, B.; Kögerler, P.; Hill, C. L. *Inorg. Chem.* **2007**, *46*, 5398.
(30) (a) Geletii, Y. V.; Botar, B.; Kögerler, P.; Hillesheim, D. A.; Musaev, D. G.; Hill, C. L. *Angew. Chem., Int. Ed.* **2008**, *47*, 3896. (b) Sartorel, A.; Carraro, M.; Scorrano, G.; De Zorzi, R.; Geremia, S.; McDaniel, N. D.; Bernhard, S.; Bonchio, M. *J. Am. Chem. Soc.* **2008**, *130*, 5006.
(31) Brese, N. E.; O'Keeffe, M. *Acta Crystallogr., Sect. B* **1991**, *47*, 192.
(32) SeeFiguerola, A.; Tangoulis, V.; Ribas, J.; Hartl, H.; Brüdgam, I.; Maestro, M.; Diaz, C. *Inorg. Chem.* **2007**, *46*, 11017 and references therein.
(33) Xin, F.; Pope, M. T. *Inorg. Chem.* **1996**, *35*, 5693.

POMs are linked by lanthanide cations has been recently published by Wang et al.[34] In the compound reported by these authors, tetranuclear Weakley-type $[Mn_4(H_2O)_2(SiW_9O_{34})_2]^{12-}$ units are connected by Ce^{III} ions. In this species, the connection of the subunits by the rare earth cations affords a single-chain monodimensional system with interchain connections ensured by alkaline counterions.

Magnetic Properties. The $\chi_M T$ vs T plot of **1** is depicted in Figure 3. The curve exhibits a continuous decrease from room temperature to 13 K, where a plateau is reached. At room temperature, the $\chi_M T$ value of 5.04 emu K mol^{-1} is lower than that expected for three uncoupled $S = 3/2$ centers ($\chi_M T_{calc} = 5.625$ emu K mol^{-1} assuming $g = 2.00$), indicating an antiferromagnetic coupling between the Cr^{III} centers. The $\chi_M T$ value of 1.76 emu K mol^{-1} at the plateau strongly suggests that the ground state is a spin quadruplet ($\chi_M T_{calc} = 1.875$ emu K mol^{-1} for a $S = 3/2$ ground state assuming $g = 2.00$). This assumption is confirmed by M vs H experiments (Figure 4), the magnetization value recorded at 2 K tending to 3 $N\beta$ (where N is Avogadro's number and β the Bohr magneton) at high fields. In a first step, the isotropic gyromagnetic factor was estimated from the $\chi_M^{-1} = f(T)$ curve, affording $g = 1.95$. As the trinuclear cluster contained in **1** adopts a nearly isosceles triangular arrangement (see above), a 2-J model has been considered for the determination of the magnetic exchange parameters (Figure 5a). The $\chi_M T = f(T)$ curve has then been fitted considering the following Hamiltonian:

$$\hat{H}(1) = -J_1(\hat{S}_{Cr1}\hat{S}_{Cr2} + \hat{S}_{Cr3}\hat{S}_{Cr2}) - J_2\hat{S}_{Cr1}\hat{S}_{Cr3} \quad (1)$$

The best fit to the experimental data in the 2−300 K temperature range with g being fixed to 1.95 afforded $J_1 = -2.6$ cm^{-1} and $J_2 = -12.0$ cm^{-1} ($R = 8.7 \times 10^{-5}$).[35] The energy diagram deduced from these values confirms the nature of the ground state, with a first excited state $S = 1/2$ located at 11 cm^{-1}.

Due to the lack of compounds possessing a $\{Cr_3(\mu\text{-}OH)_3\}$ core, no magneto-structural correlation has been proposed for such systems. Nevertheless, several studies devoted to trinuclear complexes that can be magnetically described as isosceles triangles and which possess doublet and quadruplet spin states low in energy have been reported. On the basis of considerations involving complexes possessing a $\{Mn^{IV}{}_3O_4\}^{4+}$ core ($S_{Mn(IV)} = 3/2$), it has been established that the multiplicity of the spin ground state is determined by the degree of deviation of one apical 3d ion from the plane defined by the two other 3d centers and the two oxygen atoms involved in the bridges linking the basal and apical magnetic ions. Such deviation strongly influences the J_1 coupling constant (as defined in eq 1), provoking a decrease of this parameter and then leading to small J_1/J_2 ratios. Quantitatively, it has been proposed that, for $J_1/J_2 \approx 0.4$, the doublet and quadruplet states are degenerated, while the spin ground state is $S = 1/2$ for $J_1/J_2 \gtrsim 0.4$ and $S = 3/2$ for $J_1/J_2 \lesssim 0.4$.[36]

(34) Chen, W.; Li, Y.; Wang, Y.; Wang, E. *Eur. J. Inorg. Chem.* **2007**, 2216.
(35) $R = [\sum(\chi_M T_{calc} - \chi_M T_{obs})^2/\sum(\chi_M T_{obs})^2]$.
(36) (a) Pal, S.; Chan, M. K.; Armstrong, W. H. *J. Am. Chem. Soc.* **1992**, *114*, 6398. (b) Baffert, C.; Orio, M.; Pantazis, D. A.; Duboc, C.; Blackman, A. G.; Blondin, G.; Neese, F.; Deronzier, A.; Collomb, M.-N. *Inorg. Chem.* **2009**, *48*, 10281.

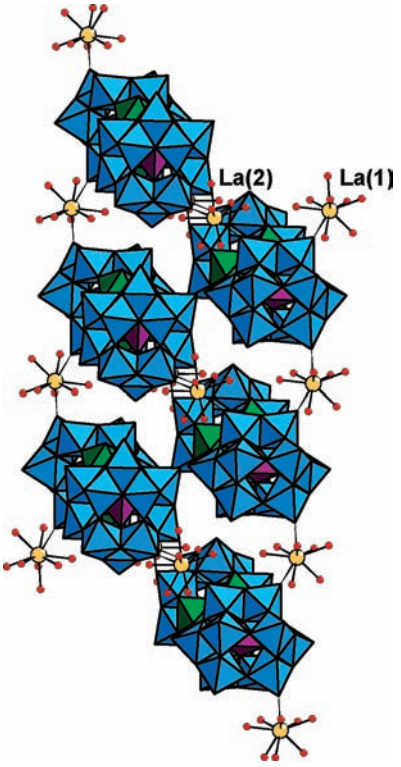

Figure 2. Polyhedral and ball-and-stick representation of the $Cs_4[(\gamma\text{-}SiW_{10}O_{36})_2(Cr(OH)(H_2O))_3(La(H_2O)_7)_2]\cdot 19H_2O$ compound **2**. Blue octahedra, $\{WO_6\}$; green spheres, Cr; yellow spheres, La; red spheres, O; purple tetrahedra, $\{SiO_4\}$.

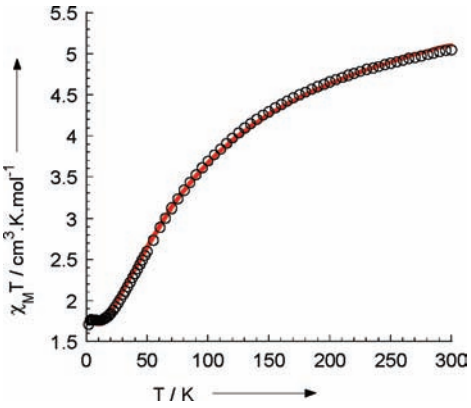

Figure 3. Magnetic susceptibility data in $\chi_M T$ form of **1**. The solid line above the experimental data is the theoretical curve derived from the Hamiltonian (eq 1, see text).

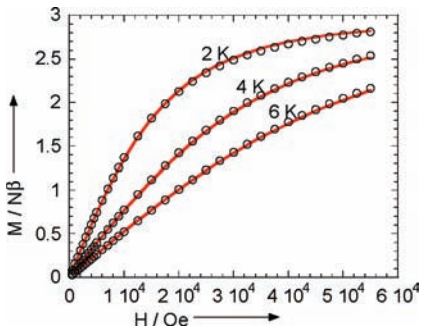

Figure 4. Magnetization vs magnetic field at 2, 4, and 6 K. The solid lines represent the best fitting results using Hamiltonian (eq 2, see text).

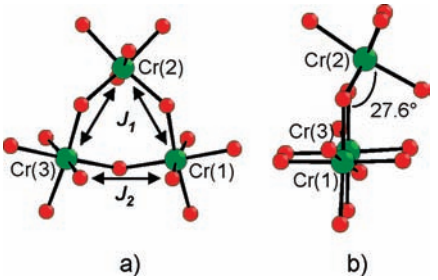

Figure 5. (a) Coupling scheme used for the fit of the magnetic data of **1**. (b) Side-on view of **1** with only the atoms directly coordinated to the Cr^{III} ions.

For complex **1**, the J_1/J_2 ratio is equal to 0.22. This is then in line with the presence of a quadruplet ground spin state. This result also agrees with the observed strong deviation of the apical Cr^{III} ion from the plane formed by the two other Cr^{III} ions and the two oxygens involved in the bridges linking the basal and apical Cr^{III} centers (27.6°, see Figure 5b). However, other examples of such systems with a $\{Cr_3(\mu\text{-}OH)_3\}$ core are required to confirm this explanation concerning the nature of the ground state and to justify the magnitude of the two exchange parameters.

The $M = f(H)$ curves recorded at 2, 4, and 6 K have also been fitted (Figure 4), considering the Hamiltonian:

$$\hat{H}(2) = \mu_B \hat{B} \cdot [g] \cdot \hat{S} + D(\hat{S}_z^2 - 1/3\hat{S}^2) + E(\hat{S}_x^2 - \hat{S}_y^2) \quad (2)$$

where D and E are the usual axial and rhombic zero field splitting (zfs) terms. The best fitting parameters are $|D| = 0.98\ cm^{-1}$, $|E/D| = 0$, and $g = 1.95$ ($R = 8.20 \times 10^{-5}$).[37] In order to check the results presented in this section, EPR experiments have been conducted.

EPR Experiments. Powder Q-band EPR spectra of compound **1** have been recorded at different temperatures. The 7 K spectrum (Figure 6) corresponds to the contributions of two spin states: $S = 3/2$ (signals at $g_{eff} = 5.63$, 4.66 and 2.66) and $S = 1/2$ (rhombic signal below $g = 2$). The increase of temperature to 20 K leads to the disappearance of the $S = 3/2$ signals, demonstrating that this spin state is fundamental and that the first excited one is a doublet. These observations are in full agreement with the energy diagram calculated from the fit of the $\chi_M T = f(T)$ curve. The electronic properties of the quartet can be described by the spin Hamiltonian $\hat{H}(2)$. The effective g values of the signals located at $g_{eff} = 4.66$ and 2.66 of the quartet notably stray from $g = 4$ and 2, respectively, values expected for the case $D > h\nu$. However, their value indicates that the magnitude of D should be comparable to the energy provided by the spectrometer ($h\nu = 1.2\ cm^{-1}$ at Q-band). The presence of a small signal at $g_{eff} = 5.63$ is indicative of $E/D \neq 0$. It results from a $|\Delta m_s| = 3$ transition within the $m_s = \pm 3/2$ Kramers doublets that have the applied field close to the z axis. The two other transitions occur between the levels $m_s = \pm 1/2$, for fields applied in the x/y and z directions for $g_{eff} = 4.66$ and 2.66, respectively. Simulation of the experimental data (Figure 6) allows the precise determination of the electronic parameters of the quartet ($D = -0.98\ cm^{-1}$, $E = -0.17\ cm^{-1}$, $E/D = 0.173$, $g_{xy} = 1.95$, $g_z = 1.93$). The D value determined by EPR spectroscopy is then in perfect agreement with that found by magnetization vs field measurements. It also agrees with our analysis that $|D| \approx h\nu$. Besides, EPR measurements revealed the rhombic character of **1**, while an $E/D = 0$ value has been found by SQUID experiments. This shows again that magnetization measurements do not allow for determining the rhombic zfs parameter. The D value of **1** is smaller than the one ($1.5\ cm^{-1}$) found for $[Cr_3(\mu_3\text{-}O)(\mu_2\text{-}C_6H_5COO)_2(\mu_2\text{-}OC_2H_5)_2(2\text{-}2'\text{-bipyridine})(NCS)_3]$ also characterized by an $S = 3/2$ ground state.[32] The negative value of D has been determined from the relative intensity of each transition and also from the g values. Indeed, it has been proposed that the sign of D is associated to g values, i.e., $D < 0$ for $g_z < g_{xy}$. The complete spectrum can be therefore simulated from the addition of the quartet and the rhombic doublet ($g_x = 2.000$, $g_y = 1.990$, and $g_z = 1.955$) spectra.

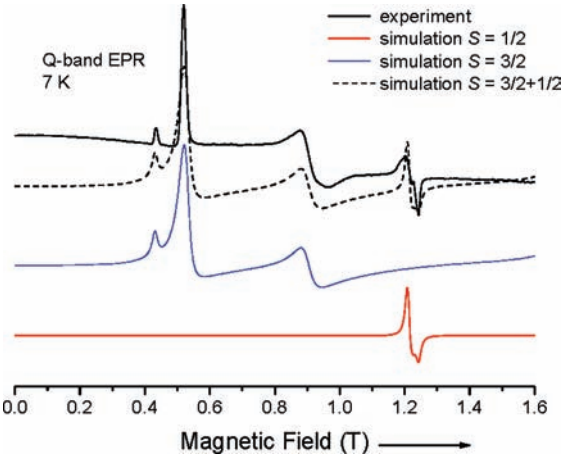

Figure 6. Experimental (black line) and simulated (red, blue, and dashed black lines) powder Q-band EPR spectra at 7 K of **1**. Parameters are given in the text.

Stability and Electrochemistry Studies. Stability studies in solution as a function of pH (from 1 to 7) was checked by UV−visible spectroscopy and cyclic voltammetry. The stability criterion was reproducibility of spectra and cyclic voltammograms (CVs) after several hours of running experiments. Complex **1** was found to be stable (more than 24 h) in solution ($[\mathbf{1}] = 10^{-4}$ M) for a wide range of pH (from 1 to 7). Such stability even at very low pH values for a hydroxo-bridged POM is not unprecedented. For example, it has been found that the $[Cu_5(OH)_4(H_2O)_2(A\text{-}\alpha\text{-}SiW_9O_{33})_2]^{10-}$ pentanuclear Cu^{II} hydroxo-bridge POM is stable in the 0−5 pH range.[38] Moreover, the pure acid salt of the $[A\text{-}\alpha\text{-}SiW_9O_{34}(Cr(OH)(H_2O))_3]^{4-}$ species mentioned in the introduction has been isolated in aqueous media in the 1.7−2.0 pH range.[10] We found that the free ligand $[\gamma\text{-}SiW_{10}O_{36}]^{8-}$ was stable enough in solution to be characterized by cyclic voltammetry under the same conditions as **1**. We were thus able to do a direct comparison between the electrochemical behaviors of **1** and its POM precursor in the four selected electrolytes.

(37) $R = [\sum(M_{calc} - M_{obs})^2/\sum(M_{obs})^2]$.

(38) Nellutla, S.; van Tol, J.; Dalal, N. S.; Bi, L.-H.; Kortz, U.; Keita, B.; Nadjo, L.; Khitrov, G. A.; Marshall, A. G. *Inorg. Chem.* **2005**, *44*, 9795.

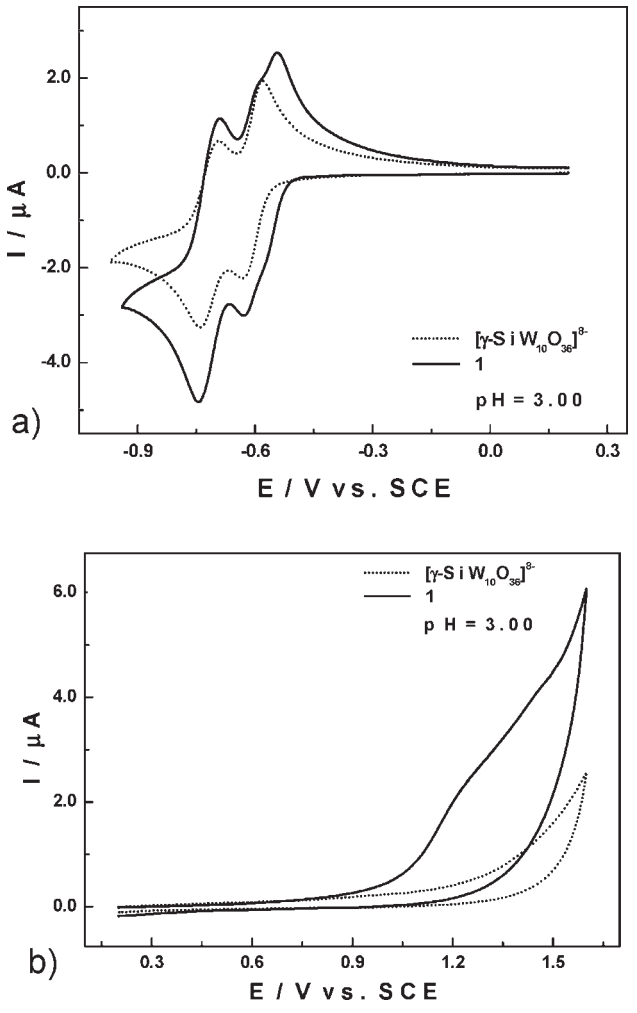

Figure 7. Cyclic voltammograms of $[\gamma\text{-SiW}_{10}O_{36}]^{8-}$ (dotted line) and **1** (solid line) in 0.2 M $Na_2SO_4 + H_2SO_4$, pH 3. Working electrode, glassy carbon; reference electrode, SCE; scan rate, 10 mV s^{-1}; polyoxometalate concentration, 0.2 mM. (a) The scanning is done in the direction of more negative potentials. (b) The scanning is done in the direction of more positive potentials.

The electrochemical behavior of $[\gamma\text{-SiW}_{10}O_{36}]^{8-}$ and **1** at pH = 3.00 (0.2 M $Na_2SO_4 + H_2SO_4$) is summarized in Figure 7. In Figure 7a, the cyclic voltammogram is restricted to the wave featuring the reduction of the tungsten framework. In fact, the voltammogram confirms that the Cr^{III} centers incorporated in the POM are not reducible to Cr^{II}.[39] The reversible reduction processes observed between −0.3 V and −0.9 V vs SCE are attributed to the reduction of W^{VI}. Although $[\gamma\text{-SiW}_{10}O_{36}]^{8-}$ and **1** CVs are very similar within this potential range, with two successive redox processes at almost the same potentials, we observe a significant difference that clearly distinguishes the two compounds. The voltammogram of $[\gamma\text{-SiW}_{10}O_{36}]^{8-}$ has the first reduction wave located at −0.620 V vs SCE followed by a second wave at −0.726 V. Both processes are reversible. The separation between the anodic peak and the cathodic peak potentials ($\Delta E = E_{pa} - E_{pc}$) is of 58 and 44 mV for the first and second waves, respectively. In contrast, the first reduction wave of **1** is clearly composite with a shoulder at −0.574 V vs SCE.

(39) Rong, C.; Anson, F. C. *Inorg. Chem.* **1994**, *33*, 1064.

Table 2. Reduction Peak Potentials, Epc, and Oxidation Peak Potentials, Epa, for the First and the Second Tungsten Waves Determined by Cyclic Voltammetry at pH 1, 3, 5, and 7 for Both Compounds $[\gamma\text{-SiW}_{10}O_{36}]^{8-}$ and Complex **1**[a]

		$[\gamma\text{-SiW}_{10}O_{36}]^{8-}$		**1**	
		Epc (V)	Epa (V)	Epc (V)	Epa (V)
pH 1	W1	−0.442	−0.406	−0.412[b]	−0.388[b]
				−0.466	−0.434
	W2	−0.552	−0.506	−0.578	−0.520
pH 3	W1	−0.620	−0.568	−0.574[b]	−0.546[b]
				−0.628	−0.594
	W2	−0.726	−0.682	−0.744	−0.690
pH 5	W1	−0.950[c]	−0.652	−0.774	−0.645
	W2		−0.840	−0.932	−0.830
pH 7	W1	−1.230[c]	−0.700	−0.878	−0.720
	W2		−0.960	−1.146	−0.950

[a] Scan rate, 10 mV s^{-1}; working electrode, glassy carbon; reference electrode, SCE. [b] There is a shoulder on the first W wave at pH 1 and 3 for **1**. [c] The two first reduction waves (W1 and W2) merge in a unique way at pH 5 and 7 for $[\gamma\text{-SiW}_{10}O_{36}]^{8-}$.

This represents a shift of + 46 mV in comparison to $[\gamma\text{-SiW}_{10}O_{36}]^{8-}$ and denotes its more basic character. The second wave remains at almost the same position (see Table 2). Controlled potential coulometry experiments were carried out in this medium (0.2 M $Na_2SO_4 + H_2SO_4$; pH = 3.00) with the potential set at −0.630 V vs SCE (potential of the first wave) leading to an average of 3.90 ± 0.05 mol of electrons consumed per mole of **1**. This corresponds to a four-electron exchange on the first wave, which is consistent with the behavior of Keggin sandwich-type complexes.[40]

Figure 7b shows CVs obtained with both compounds during scanning in the direction of positive potentials (from +0.2 to 1.6 V vs SCE reference electrode). The presence of Cr^{III} centers incorporated into the structure of **1** results in the appearance of an irreversible oxidation process located between +1.1 and +1.5 V. The irreversibility of this process is certainly due to the absorption of the oxidized system on the surface of the working electrode since it has to be polished to recover its initial "activity". The same behaviors are observed at pH = 1, 5, and 7 in the reduction of W^{VI} and in the oxidation of Cr^{III} centers, the main difference occurring in the location of the redox waves. As expected, during POM electrochemical characterization, there is a positive shift of the overall CV pattern when the pH of the medium decreases (see Figure 8).

At pH 5.00 (0.4 M $CH_3COONa + CH_3COOH$) and pH = 7.00 (0.4 M $NaH_2PO_4 + NaOH$), noticeable changes occur in the shape and the number of waves in addition to shifts of potentials. At all potentials (see Figures SI4 and SI5, Supporting Information), the cathodic and anodic currents decrease continuously as the pH increases, although the number of electrons exchanged at each wave is constant. This phenomenon is usually observed during POM redox processes in aqueous media and is directly related to protonation effects which always accompany their reduction in water.[41] In fact, the effect of

(40) Mbomekallé, I. M.; Keita, B.; Nierlich, M.; Kortz, U.; Berthet, P.; Nadjo, L. *Inorg. Chem.* **2003**, *42*, 5143.

(41) Keita, B.; Nadjo, L. Electrochemistry of polyoxometalates. *Encyclopedia of Electrochemistry*; Bard, A. J., Stratmann, M., Eds.; Wiley-VCH: Weinheim, Germany, 2006; Vol 7, pp 607−700.

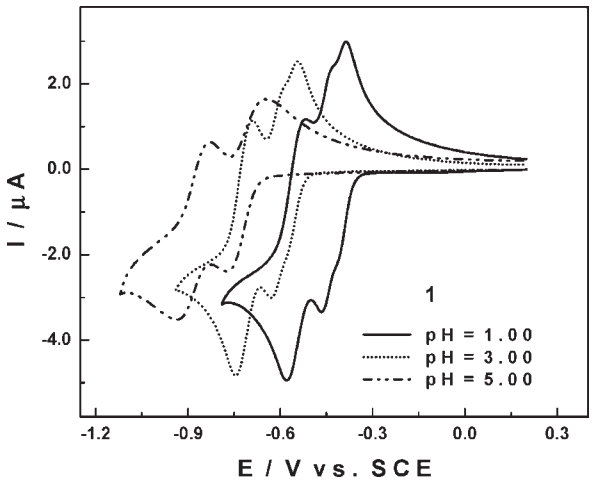

Figure 8. Cyclic voltammograms of **1** in different media. Polyoxometalate concentration, 0.2 mM; scan rate, 10 mV s^{-1}; working electrode, glassy carbon; reference electrode, SCE. pH 1 (solid line), pH 3 (dotted line), and pH 5 (dash-dotted line). CV at pH 7 was removed for better clarity of the figure but was included in Figure SI2 in the Supporting Information.

this protonation can be regarded as a catalysis by H^+, leading to an increase in current when the pH decreases.

It is also worth noting that the change observed on the first reduction process of **1** occurs at higher pH values (5 and 7 here). This wave that was composite at pH 1 and 3 now merges into a single peak at pH 5 and 7 as can be observed in Figures 8 and SI4 (Supporting Information). This is more evident with $[\gamma\text{-}SiW_{10}O_{36}]^{8-}$ where the two reduction waves observed at pH 1 and 3 completely merge into a single wave at pH 5 and 7 although the oxidation still proceeds into two distinct steps (Figure SI6, Supporting Information).

Table 2 summarizes the reduction and oxidation peak potentials associated with the first and second tungsten redox processes in the compounds $[\gamma\text{-}SiW_{10}O_{36}]^{8-}$ and **1** at pH 1, 3, 5, and 7. Oxidation potentials for the Cr^{III} centers in complex **1** cannot be defined precisely. The ranges found for each pH are given in the Supporting Information (Table SI3).

Conclusion

We have thus reported here a rare example of the Cr^{III} POM system. The $Cs_{10}[(\gamma\text{-}SiW_{10}O_{36})_2(Cr(OH)(H_2O))_3]\cdot 17H_2O$ compound **1** has been obtained starting from the trinuclear precursor $[Cr_3(CH_3COO)_7(OH)_2]$. Despite several attempts, to date, we have not been able to isolate **1** when a mononuclear Cr^{III} salt is used instead of the trinuclear unit, suggesting that the choice of the metallic precursor is crucial. We are thus currently investigating the synthesis of POM species using various chromium acetate compounds which differ by their nuclearities, sizes, shapes, and charges.[42] The physical properties of **1** have been investigated by SQUID measurements and EPR spectroscopy, revealing that in this compound the Cr^{III} ions are antiferromagnetically coupled and that **1** possesses an $S = 3/2$ ground state ($D = -0.98$ cm^{-1}, $E = -0.17$ cm^{-1}, $E/D = 0.173$). We can note that triangular Cr^{III} complexes are generally oxo-centered and that the characterization of **1** has thus provided an opportunity to investigate the magnetic exchange interactions occurring in pure μ-OH Cr^{III} triangular systems. UV−visible and electrochemical studies have shown that **1** is stable in aqueous media in a 1−7 pH range. Complex **1** can then be used as a precursor, as shown by the isolation of the $Cs_4[(\gamma\text{-}SiW_{10}O_{36})_2(Cr(OH)(H_2O))_3(La(H_2O)_7)_2]\cdot 19H_2O$ 3d−4f compound **2**. The single crystal X-ray diffraction study of **2** has revealed that, in the solid state, the rare earth cations connect these subunits, affording a double-chain monodimensional system. The use of **1** as a precursor for the synthesis of extended compounds under hydrothermal conditions is also currently under study.

Acknowledgment. This work was supported by the CNRS (UMR 5250, 8180 and 8182), the Ministère de l'Education Nationale, de l'Enseignement Supérieur et de la Recherche (MENESR), and by Grant ANR-06-JCJC-0146-01 POLYMAG.

Supporting Information Available: X-ray crystallographic files, in CIF format, for **1** and **2**; representations of the three polynuclear Cr^{III} POM complexes reported prior this work (Figure SI1); UV−visible spectra of **1** and **2** (Figure SI2); TGA of **1** and **2** (Figure SI3); cyclic voltamograms of **1** (Figure SI4 and SI5) and of the $[\gamma\text{-}SiW_{10}O_{36}]^{8-}$ ligand (Figure SI6); a table of selective bond lengths of **1** (Table SI1) and **2** (Table SI2); a table with the potential ranges for oxidation of Cr^{III} centers incorporated in **1** (Table SI3). This material is available free of charge via the Internet at http://pubs.acs.org.

(42) Eshel, M.; Bino, A.; Felner, I.; Johnston, D. C.; Luban, M.; Miller, L. L. *Inorg. Chem.* **2000**, *39*, 1376 and references therein.